CAMBRIDGE
UNIVERSITY PRESS

Key biological mechanisms involved in high-LET radiation therapies with a focus on DNA damage and repair

Zacharenia Nikitaki[1], Anastasia Velalopoulou[2], Vassiliki Zanni[1], Ioanna Tremi[1,3], Sophia Havaki[3], Michael Kokkoris[1], Vassilis G. Gorgoulis[3,4,5,6,7], Constantinos Koumenis[2] and Alexandros G. Georgakilas[1]

[1]Department of Physics, School of Applied Mathematical and Physical Sciences, National Technical University of Athens (NTUA), Zografou Campus, 15780 Athens, Greece; [2]Department of Radiation Oncology, Perelman School of Medicine, University of Pennsylvania, Philadelphia, Pennsylvania, 19104 USA; [3]Molecular Carcinogenesis Group, Department of Histology and Embryology, School of Medicine, National and Kapodistrian University of Athens, 11527 Athens, Greece; [4]Biomedical Research Foundation, Academy of Athens, Athens, Greece; [5]Faculty Institute for Cancer Sciences, Manchester Academic Health Sciences Centre, University of Manchester, Manchester, UK; [6]Center for New Biotechnologies and Precision Medicine, Medical School, National and Kapodistrian University of Athens, Athens, Greece and [7]Faculty of Health and Medical Sciences, University of Surrey, Surrey, UK

Abstract

DNA damage and repair studies are at the core of the radiation biology field and represent also the fundamental principles informing radiation therapy (RT). DNA damage levels are a function of radiation dose, whereas the type of damage and biological effects such as DNA damage complexity, depend on radiation quality that is linear energy transfer (LET). Both levels and types of DNA damage determine cell fate, which can include necrosis, apoptosis, senescence or autophagy. Herein, we present an overview of current RT modalities in the light of DNA damage and repair with emphasis on medium to high-LET radiation. Proton radiation is discussed along with its new adaptation of FLASH RT. RT based on α-particles includes brachytherapy and nuclear-RT, that is proton-boron capture therapy (PBCT) and boron-neutron capture therapy (BNCT). We also discuss carbon ion therapy along with combinatorial immune-based therapies and high-LET RT. For each RT modality, we summarise relevant DNA damage studies. Finally, we provide an update of the role of DNA repair in high-LET RT and we explore the biological responses triggered by differential LET and dose.

Introduction

The principal biophysical action of all types of ionising radiation (IR) is to eject outer (Compton effect) or inner (photoelectric effect) shell electrons from atoms or molecules (ionisation), resulting in breakage of chemical bonds. These ionisations can lead to significant damage of cellular compartments such as mitochondria, cell membranes, the endoplasmic reticulum, the Golgi complex, as well as to macromolecules, the most important being nuclear DNA (Refs 1, 2). Multiple types of DNA lesions are formed due to IR. The energy deposited in a cell by 1Gy of radiation produces approximately 10^5 ionisations or excitations, but only a small fraction (5–10%) of these events will induce permanent molecular damage in a cell nucleus (Ref. 3). Biological effects differ based on the linear energy transfer (LET) (energy and type of ionising particle) as well as the cell/tissue type. For instance, the average yield of DNA damage in a typical mammalian cell after 1Gy of high-LET radiation, consists of about 1000 base alterations, 500 single-strand breaks (SSBs), 50–70 double-strand breaks (DSBs), 3 chromosomal aberrations and 2.6 lethal lesions (Refs 3, 4). As high-LET radiations (such as α-particles and heavy ions) are densely ionising, they deposit large amounts of energy within a small distance along the track of each particle thus producing high levels of dense breaks, ROS and RNS (Ref. 5). In general, LET-increase is expected to lead to more DSBs per dose unit and increased DSB complexity (Refs 6, 7). In fact, the concept of DSB complexity was developed precisely to explain how high-LET IR can be so much more effective, without producing many more (if at all) DSBs as discussed previously in (Refs 8, 9).

Due to the nature of particle radiation, these lesions are not evenly distributed in a cell nucleus; rather, they 'cluster' along the particle track and especially towards the end. This clustering refers to the so-called concept of 'clustered lesions' which occur simultaneously at a very close distance of a few nm (Ref. 8). Of all the types of damage, clustered lesions, due to their complexity, constitute the biggest challenge for DNA repair systems. Previous studies on the processing of IR-induced DNA damage, indicated that clustered diverse lesions like DSBs, SSBs and oxidised bases will trigger the activation of several DNA repair pathways. Starting from DSBs, the erroneous non-homologous end joining (NHEJ; canonical and alternative) mechanism is believed to process the majority of DSB lesions. For cells in the S-G2 phase, the accurate and of high-fidelity homologous recombination (HR) will indeed process

DSBs. However, recent findings challenge the theory that all DSBs in S-G2 phase are processed by HR and open the door for alternative NHEJ pathways to participate in the case of highly complexed DSBs (Refs 10, 11). For all other lesions (SSBs and base lesions) base excision repair (BER) is believed to be the main player. SSB repair (SSBR) is considered a specialised, sub-pathway of BER, processing normal and abnormal strand breaks that arise either from reactions with DNA-damaging agents (endogenous or exogenous) or as intermediates in certain enzymatic events like in the processing of clustered base lesions (Ref. 9). As extensively discussed in (Ref. 12), SSBR consists of (1) strand break detection; (2) removal of 5′- or 3′-terminal blocking group; (3) gap-filling repair synthesis; and (4) nick-sealing by a DNA ligase. Two pivotal proteins orchestrate SSBR: poly(ADP-ribose) polymerase 1 (PARP1) and X-ray cross-complementing protein 1 (XRCC1) acting rather as scaffolds for the buildup of the various repair components required to mantle the SSB and restore the phosphodiester backbone.

Therefore, high-LET irradiations, even at low doses, can hobble the cellular DNA repair machinery and lead to delayed repair or misrepair, resulting in mutations and complex chromosomal aberrations (Refs 13, 14). Misrepair is usually the result of lesion proximity or choice of the DNA repair pathway (Ref. 15). For example, the repair of DSBs induced by carbon ions is dependent on resection, a process directly related to the repair pathway selected (Refs 16, 17). Misrepair is also believed to play an important role in the increased relative biological effectiveness (RBE) values after high-LET radiation compared to the low-LET one (Ref. 18).

Particle radiation therapy (RT) as a clinical modality may utilise different particles, such as electrons, protons or carbon ions; doses, such as high- and low- dose brachytherapy; dose rates, such as ultra-high dose (FLASH) RT as well as various conformality modes, such as brachytherapy, external beam RT, intensity-modulated RT and stereotactic body RT. Understanding the major advantages and disadvantages of low and high LET treatment options is of critical importance for the more accurate tumour treatment and the minimisation of toxicity in the patients. The differential level and types of biological damage induced in the tumour *versus* healthy tissues are of significant clinical importance and therefore, we will focus on the mechanisms of DNA damage induction for the high-LET RT modalities like protons, carbons, α-particle-emitting radionuclides which are highly cytotoxic and are thus promising candidates for use also in targeted radioimmunotherapy of cancer (Refs 19, 20).

Overview of medium to high-LET radiotherapies (protons, neutrons, a-particles, carbon ions)

Proton radiation therapy

Proton therapy uses a beam of protons of primarily medium LET which are positively charged particles (essentially hydrogen nuclei) with a very well-defined range of tissue penetration, to deliver radiation to a targeted tumour. Higher-LET values do exist across the track of the proton beam particularly towards the distal edge of the spread-out Bragg peak (SOBP), compared with conventional X-ray radiation (Ref. 21). This radiation modality allows for a better distribution of the delivered dose of radiation compared to photon (X-Ray) radiotherapy and has led to an expansion of the treatment options in radiation oncology. The SOBP is a combination of several Bragg peaks in such a way, that an entire tumour can be targeted with minimal dose deposition to adjacent normal tissues. The idea to use protons in cancer treatment was conceived by the physicist Robert R. Wilson in 1946 (Ref. 22) and the first patients were treated

in 1954 (Ref. 23). We have now amassed a substantial amount of clinical evidence on the efficacy of proton radiation treatment (Ref. 24). In a recent comparative analysis of protons *versus* photons in combination with chemotherapeutic regimens, proton chemoradiotherapy presented significantly reduced acute adverse events that were causing unplanned hospitalisations, with similar disease-free and overall survival (Ref. 25).

A new exciting development in the field of radiotherapy is the so-called 'FLASH' radiotherapy which has quickly evolved into a highly promising radiation modality. Proton and other particles (such as electrons or carbon ions) are delivered at ultra-high ('FLASH') dose rates (currently at >40 Gy/sec of higher) whereas in the clinic, the 'standard' dose rates are at approximately 5 Gy/min (Ref. 26). FLASH radiotherapy has demonstrated increased sparing of the normal tissue while maintaining an equipotent antitumour efficacy compared to conventional radiotherapy in multiple preclinical studies (Refs 27–34). The medium LET that characterises proton radiation, along with the SOBP can enhance the potency of 'FLASH' effect during proton radiotherapy (Ref. 26). A major advancement in the field of FLASH radiotherapy is the onset of the world's first human clinical trial of FLASH RT by the Cincinnati Children's/UC Health Proton Therapy Center. The study named as FAST-01 (FeAsibility Study of FLASH Radiotherapy for the Treatment of Symptomatic Bone Metastases) (NCT04592887), will be delivering a single radiotherapy session to the recruited cancer patients in a fraction of a second. For a recent analytical review on FLASH radiotherapy and potential biological mechanisms underlying its biological effects the reader is directed to (Ref. 26).

Carbon ion therapy

Carbon ion radiotherapy (CIRT) is another form of particle beam therapy which provides a series of physical and biological advantages (Refs 35, 36). The larger mass of carbon allows for even more reduced beam scattering, characterised by a steeper dose distribution area with minimal penumbra and sharper Bragg peak (Refs 37–39) compared to protons, theoretically allowing for better tolerance of radiosensitive organs (Refs 40–42). Moreover, carbons demonstrate higher LET than protons, something which leads to a two to three fold-higher RBE compared to protons and photons (Ref. 43) due to the more dense and complex DNA damage (Ref. 38). Other differences of CIRT compared to other radiotherapies include the lack of oxygen effect, sublethal damage repair and the reduced impact of the cell cycle on radiosensitivity (Ref. 44). Today, there are 13 CIRT centres in five countries treating tumours, such as prostate, head and neck, lung, liver, bone, soft tissue sarcomas, locally recurrent rectal cancer and pancreatic cancer (Refs 40, 45). Unfortunately, there is still scarce evidence (e.g. comparative clinical trials) comparing head-head the efficacy and toxicity of CIRT to other particle or photon RT.

Nuclear radiotherapy

The biological effects of external beam Radiotherapy are sufficiently described by the ionisation effects occurring while accelerated ions traverse and interact with the biological matter based on nuclear physics laws. Many decades ago, a combinatorial Radiotherapy modality was proposed, one where in addition to primary ionisations, accelerated particles would also cause, nuclear reactions to atoms of a suitable substrate, thus creating heavier ions (commonly α-particles), which are characterised by higher LET values. In this review, we use the term Nuclear Radiotherapy to distinguish this modality from conventional external beam RT. The adjective 'Nuclear' within the term implies

the need of nuclear physics to describe the reactions taking place, the possible nuclear energy states of implicated particles as well as their kinetic energy and finally their LET values. High LET ions are expected to cause more severe damage to the targeted cancer cells. In this review, we will focus on proton–boron (fusion/) capture therapy (PBCT) and boron-neutron capture therapy (BNCT) (see below and Supplementary data). Although initially there was a great deal of promise in the use of Nuclear Radiotherapy approaches, these have not fulfilled their promise for reasons we will outline below. A major shortcoming of Nuclear Radiotherapy has been attributed to the limited possibility of a nuclear interaction in practice. Even if an accelerated charged particle has the exact amount of energy to excite the targeted molecule/atom and its trajectory indeed points towards the target, the possibility (cross section) for the nuclear reaction to be triggered is at least 10^4 times smaller than the corresponding one for the ionisation process, even when high-energy ions or electrons are used as primary particles (Refs 46, 47). In the case of fast neutrons, an elastic and inelastic scattering are in general the dominant mechanisms for energy moderation, since human tissues act as an excellent absorber for neutron capture $(n,γ)$ reactions in the thermal (0.025 eV) and epithermal energy region (0.025–4 eV). Thus the predominant mechanisms for radiation damage and energy deposition are usually not the intended ones via the specific, useful $(n, α)$ nuclear reactions. Additionally, the delivery of adequate amounts of boronated compounds to the tumour while avoiding any significant uptake in normal tissues constitutes one of the most challenging issues for a successful treatment with the BNCT or PBCT techniques (Ref. 48). Thus, there are still many issues open for scientific investigation before the practical clinical stage is reached. Despite the clinical failure of these approaches, they have laid the foundations for a more efficacious approach based on similar principles such as PBCT (see below and in Supplementary data).

Proton–boron capture therapy

PBCT is an innovative method towards increased proton biological effectiveness. PBCT is based on pure nuclear physics principles and uses a nuclear fusion reaction between low-energy protons and ^{11}B atoms, that is

$$p +^{11}B \rightarrow {}^{12}C^* \rightarrow 3α \tag{1}$$

$$p +^{11}B \rightarrow {}^{12}C^* \rightarrow α_0 +^8 Be, {}^8Be \rightarrow 2α \tag{2}$$

$$p +^8 B \rightarrow {}^{12}C^* \rightarrow α_1 +^8 Be^*, {}^8Be^* \rightarrow 2α \tag{3}$$
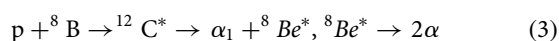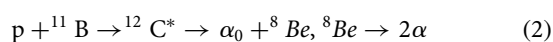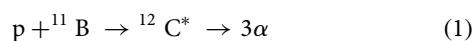
The reaction produces high LET $α$-particles of enhanced damaging potential ideally solely on the desired target tumour area that is SOBP, without damaging neighbouring normal tissues (Refs 49, 50).

Proton Boron reaction involves the production of ^{12}C in one of its excited (nuclear) states (^{12}C*). For the resonance occurring at 0.675 MeV (projectile energy) (Ref. 51) there are three main options of de-excitation. Two of them are described by the 2-step reaction ((1) and (2)) and the third by the 1-step reaction (1) (Ref. 52). According to Stave et al. the predominant one is the 2-step reaction, which involves the production of a Be nucleus (Ref. 52). In order to investigate the $α$-particles biological effects, exact knowledge of their LET is required. To calculate the LET values we need to know the energy values that they are emitted with and this can be considered as a rather complicated problem. In the following, we describe why this issue is a bit complicated.

Figure S1 (Supplementary data) illustrates the phenomenon. The p + ^{11}B → 3$α$ reaction releases an amount of energy Q = 8.59 MeV for example [http://nrv.jinr.ru/nrv/webnrv/qcalc/], which has to be shared (along with a fraction of approx. 11/12 of the incoming proton's kinetic energy) among the three ejectiles, that is the $α$-particles with varying energies as shown in Table S1 (maximum 231 keV/μm).

BNCT is a radiotherapeutic modality which targets cancer cells via a two-step procedure. During the first stage, the patient is injected with a tumour-localising drug which carries the stable isotope boron-10 (^{10}B) which has a high tendency to capture low energy 'thermal' neutrons (n_{th}). The most widely used boron delivery agents are the sodium borocaptate (BSH) and the boronophenylalanine (BPA), while the latter can be associated to fructose to yield BPA-F with enhanced solubility (Ref. 53). In the second stage, the patient is subjected to irradiation with neutrons and the subsequent nuclear reactions occurring when ^{10}B is hit with neutrons, lead to the emission of high-energy $α$-particles (^{4}He) and recoiling lithium-7 (^{7}Li) nuclei that kill the cancer cells that have accumulated sufficient quantities of ^{10}B (Refs 53–55). The basic interaction equations are described below:

$$^{10}B + n_{th} \rightarrow {}^{11}B^* \rightarrow α_0 +^7 Li \tag{4}$$

$$^{10}B + n_{th} \rightarrow {}^{11}B^* \rightarrow α_1 +^7 Li^* \tag{5}$$
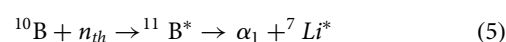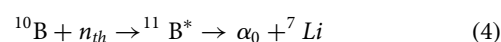
Using catkin 2.03 and jinr Q-value_calc [http://nrv.jinr.ru/nrv/webnrv/qcalc/] one can easily determine the levels of the kinetic energy of implicated particles, considering for neutrons T_n = 0.025 eV:

$$T_{α_0} \text{ is } 1.776 \text{ MeV while } T_{Li} = 1.014 \text{ MeV } T_{α_1}$$
$$= 1.472 \text{ MeV and } T_{Li*} = 0.840 \text{ MeV}$$

Figure S2 (Supplementary data) illustrates the energy levels implicated in boron-neutron fusion. The major benefit of this approach is the protection it affords to critical normal tissues from radiation-induced damage, even at the margins of the tumour (Ref. 54). This supports the use of BNCT as an alternative therapeutic option for the treatment of multiple, locally invasive malignant tumours such as high-grade gliomas (Ref. 56), recurrent cancers of the head and neck region (Ref. 57) and primary tumours or cerebral metastases of melanoma (Ref. 58). Current clinical evidence mostly revolves around the use of non-radioactive ^{10}B. Gadolinium-157 (Gd), another non-radioactive isotope has also been used but the present data have been strictly derived from in vivo studies without further examination of its efficacy in the clinic (Refs 59–61).

There are prerequisites for the ideal boron-containing candidate such as low systemic toxicity, much higher tumour uptake compared to the normal tissue and rapid clearance from normal tissues. Currently, the most successful boron delivery agent, BPA selectively accumulates in tumours through cancer-related amino acid transporters including LAT1 (Ref. 62). However, this approach also carries disadvantages such as reduced solubility and a short retention time (Ref. 63). The demand for better tumour targeting properties and a noticeable difference in the rate of uptake of boron-containing agents by different patients, have ushered in the production of several generations of boron-containing agents including boron-containing porphyrins, amino acids, polyamines, nucleosides, peptides, monoclonal antibodies, liposomes, nanoparticles of various types, boron cluster compounds and co-polymers (Refs 53, 55, 64–67). The current list of malignancies for which BNCT has shown at least some

clinical benefit is quite long (Ref. 48) and includes glioblastoma multiforme (Refs 56, 68–70), meningioma (Ref. 71), head and neck cancers (Refs 57, 72–76), lung cancer (Ref. 77), sarcomas (Ref. 78), cutaneous malignancies (Refs 79–81), extramammary Paget's disease (Ref. 58), paediatric cancers (Refs 82–84) and metastatic disease (Refs 85, 86). These studies underscore the promise of PBCT as a therapeutic strategy, especially for radiotherapy-resistant tumours. Moreover, if coupled with proton FLASH radiotherapy modalities, BPCT could further enhance the proton therapy therapeutic index. (Ref. 49).

Alpha-particle emitter radiopharmaceutical therapy (α-RPT)

Cancer therapy based on α-particle radiopharmaceutical emitters is a relatively new technological advancement and clinical modality with only a few such drugs available in the market for clinical use (Ref. 87). α-particles emitted from radionuclides have a high LET (>100 keV/μm) which produces a short, highly dense track of ionisation events within cellular targets, leading to repair-resistant complex DNA damage and more effective cell killing compared to sparsely ionising forms of radiation, such as γ- or X-rays. Moreover, based on well-known radiobiology from the 1980s, alpha-emitting radionuclides exhibit a high RBE for cell killing (as high as 8) (Ref. 88) accompanied by a significantly reduced dependency on hypoxia which is responsible for solid tumour radioresistance (Ref. 89). Currently, drugs being used in patients or under clinical trials are based on ^{223}Ra and ^{224}Ra as α-particle emitters (Diffusing Alpha Radiation Emitters Therapy; DaRT). A search in NCI clinical.trials.gov on 21/11/2021 using the keywords 'alpha emitters' or 'alpha particle emitter' or 'alpha radiation emitter' retrieved a maximum of 19 studies for treating resistant prostate or breast cancer with metastases as well as skin and soft tissue tumours. Radium-223 dichloride (Xofigo®, Bayer HealthCare Pharmaceuticals Inc.) is the first α-RPT approved by the FDA, with benefits in overall survival and delay in symptomatic skeletal events for patients with metastatic castrate-resistant prostate cancer (CRPC). Recently, an automated bone scan algorithm has shown its value in determining the response to radium-223 (Ra-223) treatment for patients with metastatic CRPC (Ref. 90).

DNA Damage (DSB, SSBs) involved in each high-LET modality

Proton Based therapies

Proton therapy is a quickly expanding radiotherapy modality where accelerated proton beams are utilised to accurately transport their maximum of energy and dose to the tumour but is usually ineffective against highly radioresistant tumours. In the case of protons, typical energies used in the clinic regularly range from 60–250 MeV including the case of the latest advances in the field that is, the FLASH method where ultra-high dose rates 40–200 Gy/s can be achieved through the delivery of very short proton ms-pulses (Refs 91, 92).

Theoretical considerations

In an effort to have a better understanding of the primary molecular effects of high-LET radiations, we have mined accumulated data on the induction rates of double and single-strand breaks (DSBs and SSBs respectively) for a variety of biological systems and both experimental and simulation data (Tables 1–3). Theoretical predictions of biological damage from DNA to cellular survival are always very helpful and have aided significantly the planning of experiments and interpretations of results. By the word of theoretical predictions, we refer to the well-accepted and acknowledged stochastic modelling using Monte Carlo

(MC) simulations and particle track structure codes [for recent reviews please see (Refs 93, 94)] as well as others non-stochastic using mathematical or machine learning-based calculations (Refs 95–97). It must be mentioned though that all simulations of any type are optimised based on experimental data. For example, using the Geant4DNA MC code and an improved DNA geometry model as well as clustering algorithms, DNA damage yields were calculated and compared to literature (Ref. 98). The model was tested against published experimental and computational results for DSB rates and RBE values. A general agreement was observed over the whole simulated proton energy range. The DSB yield was 8.0 ± 0.3 DSB Gy^{-1}Gbp^{-1} for ^{60}Co, and 9.2 ± 0.2 DSB Gy^{-1}Gbp^{-1} for 250 kVp X-rays, and between 11.1 ± 0.9 and 8.1 ± 0.5 DSB Gy^{-1}Gbp^{-1} for 2–100 MeV protons. The specific results suggest that DSBs consist of direct and indirectly-induced (through ROS) SSBs that account approximately for half of the total DSBs (Ref. 98).

Table 1 contains data from in vitro and in silico works using protons and electromagnetic irradiation. Variations among different simulations can be attributed to different initial conditions fed into the algorithm, and especially the concentration of antioxidants, oxygen levels and nuclear DNA density. As a general conclusion, it can be deducted that an increase in LET leads to an increase of DSBs and to a reduction of SSB levels as well as of other non-DSB oxidative damage (Refs 98–101). This of course suggests a higher level of complexity for DSBs at least.

Carbon Ion radiotherapy

CIRT is the treatment of choice for proton-resistant tumours like sarcomas (Ref. 35). Table 2 contains data from in vitro and in silico studies of carbons. Keta *et al.* (Ref. 102) irradiated three malignant cell lines with protons or carbons and they evaluated DNA damage by quantifying γH2AX foci. No significant differences were observed in the γH2AX foci formation between the two radiation modalities and they attributed this result to the limited resolution that ICC offers when performed using conventional fluorescence microscopy. Yokota *et al.* (Ref. 105) using pulsed-field gel electrophoresis (PFGE) quantified DSBs yields in protoplasts from the tobacco BY-2 cell line. They identified a difference in the induced DSB between γ-rays and carbon ions, but they could not satisfactorily detect a difference in the DSB yields among the several LET values of carbons. Moreover, their approach failed to exhibit expected results that is higher DSBs for the highest LET used. They interpreted this result by the phenomena occurring to the carbons penumbra region and to the possible dosimetry inaccuracies. Back in 1995, Heilmann *et al.* (Ref. 106) irradiated CHO-K1 cells with carbons of different energies and assessed DNA damage using constant-field gel electrophoresis. Their results, although not revealing an increased number of DSBs, underline the possible inability of electrophoretic approaches to detect very small DNA fragments as a result of highly complex DSBs, a phenomenon also discussed in (Ref. 8). Shiina *et al.* (Ref. 107) compared carbons of 60 keV/μm LET and X-rays using agarose gel electrophoresis (AGE), in several Tris scavenger concentrations. Comparing results for minimum (1.0×10^6/s) and maximum (Tris 1.0×10^{10}/s) scavenging capacities of Tris. Corresponding values of Tris scavenging capacity that mimics cellular environment, that is 3.0×10^8/s are also presented in Table 2. An increase in scavenging capacity causes a decrease of both DSB and SSB levels, for every radiation modality.

α-particles Produced during nuclear radiotherapy

α-particles are produced during nuclear radiotherapy as well as during brachytherapy. They have short ranges in the body,

Table 1. Protons and electromagnetic irradiation

Radiation	LET (keV/μm)	Model system		DSBs/(Gbp*Gy)	SSBs/(Gbp*Gy)	Ref
2 MeV ^{1}H		Simulations		11.1	~130	(Ref. 98)
100 MeV ^{1}H				8.1	~142	
250kVp X-rays				9.2	199	
^{60}Co γ-rays				8.0	208	
^{1}H	39.7	Simulations		7.8	39	(Ref. 99)
	24.2			7.77	51	
	13.9			6.36	63	
	3.4			4.3	73	
	1.9			3.5	75	
^{1}H	22.6	Mammalian cells -Simulation		12	170	(Ref. 100)
	18			11	175	
	11.9			10	178	
	7			9	183	
	4.02			9	184	
	1.11			8	187	
^{60}Co γ-rays	2.4			8	–	
^{1}H	30.2	Nucleosome structures of 198 DNA bp Simulation		6.22	64.65	(Ref. 101)
	28.2			6.03	65.19	
	24.7			5.68	66.5	
	22.2			5.53	67.61	
	19.2			5.27	68.9	
	12.2			4.64	71.4	
	11.1			4.56	71.71	
	8.7			4.33	72.8	
^{60}Co γ-rays	0.3			3.50	74.8	
^{1}H	4.4	HTB140 melanoma		4.3		(Ref. 102)
		MCF-7 breast adenoca.		4.5		
		HTB177 non-small l. ca		4.7		
^{60}Co γ-rays	0.3	HTB140 human melanoma		2.6		
		MCF-7 breast adenocarcinoma		3.2		
		HTB177 non-small l. ca		3.5		
^{1}H	1.051	Mammalian	w/o DMSO	8	187	(Ref. 103)
		cells-Simulation	64 mM DMSO	5	149	
			1 M DMSO	3	110	
^{60}Co γ-rays	0.3	HTB140 human melanoma				
		MCF-7 breast adenocarcinoma				
^{1}H 0.05 Gy/sec	2.3	pBR322 plasmid DNA solution		27	2476	(Ref. 104)
40 Gy/sec		(4361 bp, 0.5 μg/μl in 1 × TE)		25	2016	

depending on their emission energy, usually less than 100μm. Their energy and consequently their LET change dramatically with distance, when traversing tissues or water, which is considered roughly radiologically equivalent to tissue. Table 3 includes studies using plasmid DNA, protoplasts, cells or simulations: Pater *et al.* (Ref. 101) using MC simulations observe similar dependence of DSB and SSB with LET for α-particles and for protons: LET increase leads to DSB increase against SSB levels which decrease. Yokota *et al.* (Ref. 105) counted DSB yields after exposure to α-particles or γ-rays, by using protoplasts from the tobacco

BY-2 cell line and by performing PFGE: LET increase resulted to increase of DSB levels. In another study, by using plasmid pUC18 and AGE, it was found that LET increase leads to an increase of DSB yields but it was not detected to affect the number of SSBs per Gy and per Gbp (Ref. 110). Prise *et al.* (Ref. 111) compared α-particles and γ-rays irradiation using pNSG-CAT plasmid and AGE at two concentrations of the ROS scavenger Tris. At both concentrations, similar results with (Ref. 101) for both scavenging conditions were acquired. A study using V79-379A hamster cells and PFGE shows increased DSB levels for α-irradiation compared

Table 2. Carbons and electromagnetic radiations

Radiation	LET (keV/μm)	Model system		DSBs Gbp^{-1} Gy^{-1}	SSBs Gbp^{-1} Gy^{-1}	Ref
^{12}C	199	HTB140 melanoma		4.8		
		MCF-7 breast adenoca.		4.2		
		HTB177 non-small l. ca		4.6		
^{60}Co γ-rays	0.3	HTB140 human melanoma		2.6		(Ref. 102)
		MCF-7 breast adenocarcinoma		3.2		
		HTB177 non-small l. ca		3.5		
^{12}C	431	Protoplasts from the tobacco BY-2 cell line (12.3 Gbp/diploid)		2.43		
	241			5.11		(Ref. 105)
	124			5.19		
	94.8			4.81		
^{60}Co γ-rays	0.2			3.15		
^{12}C	400	CHO-K1 cells		5		
	228			6		
	154			10		(Ref. 106)
	103			15		
	17			16		
	14			14		
Xrays	2			15		
^{12}C	60	pUC18 plasmid DNA (2686 bp)	Tris 1.0×10^6/s	169*	3380	(Ref. 107)
			Tris 3.0×10^8/s	18.2	176	
	13		Tris 1.0×10^6/s	228	5590	
			Tris 3.0×10^8/s	13	325	
			Tris 1.0×10^{10}/s	7.8	104	
X-rays			Tris 1.0×10^6/s	110	5720	
			Tris 3.0×10^8/s	7.8	162	
			Tris 1.0×10^{10}/s	10.4	124	
*results in (Ref. 107) are given per Da; we have converted them per bp by using a factor of 650						
^{12}C	450	Simulation: linear B-form DNA segment of 150-bp length scavenging capacity 3.24*10^8 s^{-1}		35	191	(Ref. 108)
^{12}C	60–80	Peripheral blood samples, collected from healthy donors		1.1		(Ref. 109)
X-rays				1.9		

to X-rays (Ref. 112). To summarise, all the studies show that the LET increase leads to DSB increase against SSB, at least for moderate LET values.

Overview of DNA repair pathways involved in each high-LET radiotherapy 4.1. The role of DNA repair in high-LET radiotherapy
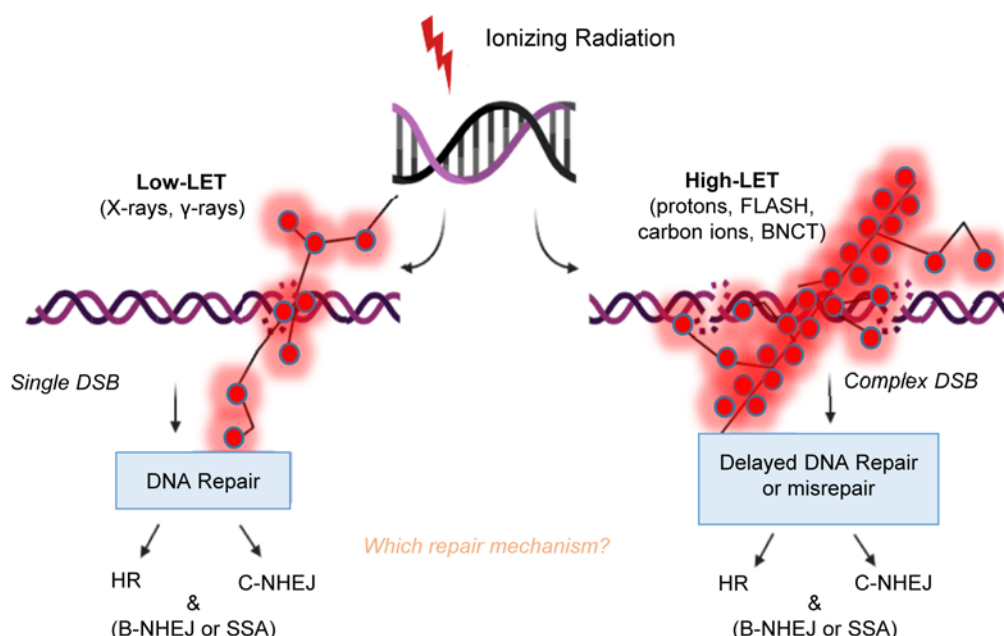
Cellular damage response pathways are expected to be activated even after the induction of low levels of biological damage in DNA, proteins or lipids (Refs 115, 116). Although, we acknowledge here the importance of damage to protein and lipids by IR, we give emphasis to the damage induced to genetic material and specifically, DNA. To mitigate threats on genome integrity posed by genotoxic agents like high-LET radiations, cells have evolved a complex set of repair mechanisms collectively called the DNA Damage Response (DDR) (Ref. 115). DDR coordinates DNA repair, DNA replication, and cell-cycle checkpoint pathways with cell fate, including apoptosis and senescence. Various DNA repair mechanisms are engaged for the processing of DNA damaged sites, especially the repair of DNA DSBs. DNA repair pathways of mammalian cells, include the BER, the nucleotide excision repair (NER), the mismatch repair (MMR) as well as the pathways responsible for the repair of DSBs, which are the HR, the classical non-homologous end joining (c-NHEJ), the backup non-homologous end-joining (B-NHEJ) and single-strand annealing (SSA). The choice of the repair pathway for DNA DSBs primarily depends on radiation quality (Ref. 117) and possibly on DSB load (Ref. 10). The induction of DNA lesions of diverse and varying levels of complexity is expected to trigger simultaneously different DNA repair pathways. Currently, it is not yet clear if there is a preference in the choice of repair pathway between low-LET and high-LET radiation (Fig. 1) (Ref. 118).

In general, isolated DSBs induced by low-LET radiation are mainly repaired by c-NHEJ and HR, while clustered DSBs generated by high-LET radiation are difficult to repair (Ref. 119).To

Table 3. α-particles and electromagnetic radiations

Radiation	LET (keV/μm)	Model system		DSBs Gbp^{-1} Gy^{-1}	SSBs Gbp^{-1} Gy^{-1}	Ref
^{4}He	29.3	Nucleosome structures of 198 DNA bp; simulation		5.51	67.0	(Ref. 101)
	24.2			5.19	68.8	
^{4}He	17.7	Protoplasts from the tobacco BY-2 cell line (12.3 Gbp/diploid)		4.89		(Ref. 105)
	9.4			4.42		
^{60}Co γ-rays	0.2			3.15		
^{4}He	95	Plasmid DNA (pUC18, 2686 bp) AGE		7.09	43.81	(Ref. 110)
	63			4.87	46.86	
	19			2.4	44.53	
^{238}Pu α-particles	110	Plasmid pMSG-CAT DNA AGE	10 mM Tris	25	200	(Ref. 111)
			200 mM Tris	15	76	
^{60}Co γ-rays			10 mM Tris	15	710	
			200 mM Tris	7	420	
^{211}At α-particles	110	V79-379A hamster cells PFGE		22		(Ref. 112)
X-rays				7		
^{4}He	14.5	SV40 DNA		617	11 483	(Ref. 113)
X-rays	1.87			572	12 094	
^{60}Co γ-rays	1			596	14 687	
^{238}Pu α-particles	120	pUC18 plasmid		14	106	(Ref. 114)
^{60}Co γ-rays				11	370	
^{238}Pu α-particles	120	V79 cells		10	46	
^{60}Co γ-rays				8	191	

Fig. 1. Double-strand breaks (DSBs) repair pathways after low- and high-LET radiation. Protons maybe considered medium to high-LET only towards the distal end of their track.

examine the effects of radiation on DNA DSB repair and radio-sensitivity, Takahashi *et al.* used embryonic fibroblasts bearing repair gene (NHEJ-related Lig4 and/or HR-related Rad54) knockouts (KO) and showed that c-NHEJ plays a more essential role compared to HR in defining radiosensitivity after high-LET (carbon ions) radiation (Ref. 120). This implies that c-NHEJ might be the principle repair mechanism used in response to high-LET IR-induced DSBs. Another study from Okayasu *et al.* showed that the clustered DSBs induced by high-LET (heavy ions) radiation may markedly depend on c-NHEJ (Ref. 121). Sridharan *et al.* further supported this hypothesis by showing that Artemis, a key complex of c-NHEJ is involved in the repair of

the clustered DSBs induced by high-LET radiation (Ref. 122). In addition to the c-NHEJ and HR pathways, residual simple and clustered DSBs induced by IR can also be repaired by the pathways of alt-EJ and SSA, but the detailed processes of the two pathways in response to high- and low-LET radiation are still unclear (Ref. 10). Even though high-LET IR induces DNA damage complexity, DSBs induced by $^{56}Fe^+$ ions are actively processed, compared to low-LET IR (e.g. X-rays) albeit with a somewhat reduced efficiency (Ref. 123). Again, this leads to the conclusion that a significant amount of high-LET IR-induced DSBs is processed by c-NHEJ.

In contrast to the notion that c-NHEJ maybe the preferable pathway for lesions of increased complexity stated above, there are studies that support the idea that the HR pathway may be favoured for the repair of heavily charged particle-induced clustered DNA lesions. For instance, Zafar *et al.* propose that complex DSBs generated by high LET irradiation from very high-Z particles are repaired by HR and not NHEJ in mammalian cells (Ref. 124). Other studies with protons also support this notion (Refs 125, 126), since mammalian cells deficient in HR factors such as Rad51 paralogs are sensitive to heavy particle radiation (Ref. 124). Interestingly, most studies that suggest a major role for NHEJ in the repair of DNA damage, are mainly carbon ion-based studies (Ref. 127). Ariungerel *et al.* suggest that the NHEJ pathway plays an important role in repairing DSBs induced by both clinical proton and carbon ion beams (Ref. 128). However, they propose that in the case of carbon ions, the HR pathway appears to be involved in the repair of DSBs to a greater extent compared to gamma rays and protons. Recently, c-NHEJ has also received strong interest in BNCT-induced damage (Refs 38, 129). Kondo *et al.* showed that DNA damage induced by BNCT is partially repaired by a key player of the NHEJ pathway, ligase IV (Ref. 129). Another study on human thyroid follicular cancer cell line (WRO) demonstrated that after BNCT, HR is the main activated pathway based on high expression of Rad51 and Rad54, while in the human melanoma cell line (Mel J) both, the c-NHEJ and HRR pathways were activated (Ref. 130).

In vitro experiments in A549 cells, have shown that there is no difference in the initial formation (within 15–30 min) of γ-H2AX foci between low- (γ-rays) and high-LET (carbon ions) radiation (Ref. 131). However, when the DNA damage repair is investigated at later time points, it shows delayed or less complete repair of DSBs in case of high-LET radiation (Refs 132, 133). Recently, the cellular responses in terms of DNA damage and repair efficacy after a mixture of radiation beams have gained interest. (Ref. 50). In the clinic, cancer patients treated with proton and carbon beams are exposed to mixed radiation fields of, that is to high-energy nuclear particles which, based on nuclear interactions, produce low-energy secondary particles (for example electrons) of high-LET that contribute considerably to overall radiation effects (Ref. 134). Many therapies besides BNCT, such as intensity-modulated radiotherapy (IMRT), proton therapy, and hadron therapy also produce mixed fields of radiation (Ref. 135). Experiments using neutron and gamma rays mixed fields showed some minor differences compared to single neutron or gamma radiation exposures (Ref. 136). While results on mixed irradiation with α-particles and X-rays show an increased amount of DNA damage (above the combined additive outcome) and delay in repair, which substantiate the idea that exposure to mixed beams presents a challenge for the DDR (Ref. 137).

The Role of apoptosis, autophagy, necrosis and senescence in high-LET radiotherapy

Cells exposed to IR can exhibit a multitude of responses. Depending on the radiation type, LET (low- or high-), dose, dose rate and radiosensitivity of the exposed cell type, IR may induce cell death through apoptosis, autophagy or necrosis, mitotic catastrophe or even cell cycle arrest and accelerated senescence (Ref. 138). For most cancer cell types, mitotic catastrophe is the most common end result of IR, whereas apoptosis (programmed cell death) is associated primarily with hematopoietic cancers (Refs 139, 140) which have a lower apoptotic threshold. The primary aim of RT is to clonogenically kill cancer cells, causing the minimum disruption to healthy ones; (Refs 141, 142). Apoptotic pathways after IR have been defined and these are the membrane stress pathway, the intrinsic pathway and the extrinsic pathway (Ref. 143). Different studies for example on the head and neck cancer underline the differences between cell death mechanisms for low or high-LET radiation therapies (for a recent review please see (Ref. 144)).

The intrinsic pathway of apoptosis is mediated by DNA SSBs and DSBs. When DNA lesions are repairable, the emerging growth arrest is transient, eventually resulting in DNA repair, cell cycle continuation, and a return to cell replication and growth. In contrast, when DNA lesions are severe or irreparable (e.g. severe DNA damage or complex damage), prolonged DDR signalling is triggered, resulting in apoptosis or senescence (permanent growth arrest) (Ref. 145). The extrinsic pathway on the other hand, involves signalling through death receptors (DRs), which belong to the tumour necrosis factor (TNF) receptor superfamily. The accumulation of p53 is critical to IR-induced apoptosis or senescence (Ref. 146). Several target genes of the p53 transcription factor encode proteins, such as p21 and p27 that induce cell-cycle arrest, PAI1 and CDKN1b which are involved in the induction of senescence, or PUMA, BAX and NOXA which are mediators of apoptosis (Ref. 147). Most solid tumour cells have either inactivating p53 mutations or defective apoptotic machinery, which makes them radioresistant and might affect the response to RT (Refs 148, 149). Necrosis, another type of cell death, is an outcome usually appearing in response to very large doses of radiation (>55 Gy), although as a rare side-effect (Ref. 150). There are cases though, that even doses as low as 2–4 Gy can cause significant necrosis. Most replicating cells die by the mitotic catastrophe which mistakenly some researchers equate to necrosis [the reader can consult this seminal review (Ref. 151)].

It may occur in lower doses as well, but it is often viewed as an unregulated event. Autophagy is a mechanism responsible to maintain metabolic homoeostasis through the segregation of damaged or unwanted cytoplasmic constituents into autophagosomes, destined for lysosomal degradation. Autophagy is directly correlated to the DDR, since there is evidence that is activated by DNA damage and is required for several functional outcomes of DDR signalling, including repair of DNA lesions, senescence, cell death and cytokine secretion (Ref. 152). In response to IR, it is yet unclear whether autophagy promotes cell survival or cell death (Refs 153–155) although it could be either of the two depending on cell context and dose. Senescence is the process by which cells irreversibly stop proliferating and enter a state of permanent growth arrest (Ref. 156). IR has been shown to induce senescence especially via the induction of DNA damage. Understanding the mechanisms that result in one of the above cellular responses is extremely important especially for an effective RT. Patients that have received stereotactic body radiation therapy (SBRT), frequently experience recurrence [e.g. non-small cell lung cancer (NSCLC) patients, stage I], reducing the overall effectiveness of radiotherapy effective (Ref. 157). It has been postulated that tumour recurrence is can derive from senescent transformed cells in the tumour area which reverse or escape the senescent phenotype (Ref. 158).

Due to the importance of RT induced-cell death, many studies have been performed with proton, carbon and even FLASH

radiation in an attempt to improve the efficacy of RT. For example, Zhang *et al.* showed that irradiation of chemoresistant cancer stem cells (CSCs) with 4Gy of protons significantly lowered cell viability, invasiveness and a number of tumour spheres compared to gamma rays. This effect was accompanied by increased apoptosis and higher ROS level (Ref. 159). In general, there is an agreement in the literature that proton radiation causes increased levels of apoptosis than photon radiation (Refs 141, 159, 160). Miszczyk *et al.* investigated the rate of cell killing by apoptosis or necrosis in human peripheral blood lymphocytes and found that irradiation with 60 MeV SOBP caused higher levels of cell death compared to 250 kV photons through necrosis (Ref. 161). Wang *et al.* assessed cell death in four HNSCC cell lines after a single dose of 4 Gy 6 MV photons or 200 MeV SOBP protons and didn't find any differences between the levels of necrosis and apoptosis. They did however, observe increased senescence and mitotic catastrophe following proton irradiation (Ref. 162). These differences can be attributed to the different cell types used for the experiments. Normal human diploid lung fibroblasts exposed to FLASH dose rate protons, showed that proton dose rate did not influence cell killing, but by increasing the dose or the dose rate they reported different rates of senescence. After they exposed cells to 20 Gy 4.5 MeV protons, they found that compared to 0.05 Gy/s, the FLASH dose rates of 100 Gy/s or 1000 Gy/s led to a reduced number of senescent cells (Ref. 163). Han *et al.* used FLASH radiation (~10^9 Gy/s, with doses in the range of ~10–40 Gy) on normal mouse embryonic fibroblast cells and analysed early apoptosis, late apoptosis and necrosis of cells under both normoxic and hypoxic conditions (Ref. 164). Their results showed that FLASH-IR compared to conventional proton therapy induced significant early apoptosis, late apoptosis and necrosis, and the levels of apoptosis increased with time, in either hypoxic or normoxic conditions. Also, in hypoxic conditions, apoptosis and necrosis were significantly lower. As also shown conclusively in Table 4, in most cases, protons induce mainly apoptosis and not necrosis. This could impact radiotherapy because cells undergoing necrosis lose membrane integrity and leak their intracellular components some of which serve as danger signals that stimulate inflammation and strong innate immune responses (immunogenic cell death) (Ref. 165) impacting tumour radiosensitisation and radiation toxicity (Ref. 138).

Atsushi *et al.* irradiated human glioma cells (NP-2), with carbon ions and found that at 6 Gy the majority of the cells die by apoptosis and autophagy. The residual cells could not form a colony and showed a morphological phenotype consistent with cellular senescence (Ref. 142). The detection of senescent cells was also confirmed with SA-β-gal staining. The same group also found that irradiation with carbon ions induced cellular senescence in the same cell line lacking functional p53. Finally, one study has provided significant data in response to carbon ion radiation and autophagy, implying that targeting autophagy might enhance the effectiveness of heavy-ion radiotherapy (Ref. 173). They also found that by inhibiting autophagy apoptotic cell death was accelerated, resulting in increased radiosensitivity. The biological cell death effects discussed in this section are summarised below in Table 4.

Combinational therapies with high-LET and immune therapies

Radioimmunotherapy aims at delivering radioactive atoms that emit beta particles, alpha particles and Auger electrons to tumours after chemically conjugating the radionuclides to monoclonal antibodies which recognise specific receptors and tumour antigens (Refs 174–176). The variable physicochemical properties of radionuclides such as half-lives and path lengths can be harnessed for the delivery of more personalised therapy and have rendered radioimmunotherapy a burgeoning field of research in the past thirty years. There is a plethora of data derived from animal tumour models using different radionuclides and monoclonal antibodies. Two radioimmunotherapeutic agents, 131I-tositumomab (Bexxar) and 90Y-ibritumomab tiuxetan (Zevalin), have been approved by the US Food and Drug Administration (FDA) (Refs 177, 178) for the treatment of CD20$^+$ B-cell lymphomas and Zevalin has also been approved by European Medicines Agency in 2000 (Ref. 179). Despite their clinical efficacy, neither has been broadly utilised in clinical practice due to financial and logistic issues. The recently added arrow into the radio-immunotherapy quiver is the US FDA and European Medicines Agency (EMA) approved 177Lu-oxodotreotide (177Lu-DOTA-Tyr3-octreotate, 177Lu-DOTA-TATE, Lutathera). LUTATHERA is a radiolabeled somatostatin analogue and was designed for the treatment of somatostatin receptor-positive gastroenteropancreatic neuroendocrine tumours (GEP-NETs) (Ref. 179).

The clinical success of the radioimmunotherapy agents has yet to be matched for the treatment of solid tumours as most of the monoclonal antibodies are conjugated to low LET β-particle emitters such as ^{131}I, ^{177}Lu or ^{90}Y (LET = 0.1–1.0 keV/μm) which are less potent (Ref. 175). Moreover, β-particle emitters pose dose-limiting normal tissue toxicity to the hematopoietic system due to their wide (2–10 mm) range. However, it has been postulated that toxicity to the bone marrow could potentially be avoided with the use of antibodies conjugated to α-particles emitters (e.g. ^{225}Ac, ^{213}Bi, ^{212}Pb or ^{211}At) and Auger electron emitters (e.g. ^{111}In, ^{67}Ga, ^{123}I or 125I) due to their smaller ranges (28–100μm for a-particles and nanometres for Auger electrons). It has also been hypothesised that the higher LET of α-particles and Auger electrons (50–230 keV/μm and 4 to 26 keV/μm, respectively) can shift radioimmunotherapy towards higher anti-tumour efficacy (Ref. 175). The exploration of the properties of α-particles and Auger electrons as well as the testing of their antibody-conjugated emitters on animal tumour models have been thoroughly reviewed by Aghevlian *et al.* (Ref. 175). Prostate cancer (Refs 180, 181), disseminated lymphomas (Ref. 182), ovarian cancer (Ref. 183), brain tumours (Refs 181, 184), mammary carcinoma (Ref. 185), glioma xenografts (Ref. 184), colon cancer xenografts (Refs 186–189), leukaemia (Refs 190, 191), breast cancer (Ref. 192) are some of the malignancies that have been treated with radioimmunotherapy using high LET α-particle and Auger electron emitters. Importantly, these findings have resulted in the initiation of several Phase I clinical trials for patients with advanced myeloid leukaemia (ClinicalTrials.gov Identifier: NCT00672165 and NCT01756677) with malignant gliomas (Ref. 193) and ovarian cancer (Refs 194–196).

Conclusions

Particle radiotherapy (RT) and hadron / ion-therapy have substantially advanced the practice of radiotherapy which has traditionally relied on the use of photons. The beneficial potential of particle RT stems from the physical properties of charged particles and the essence of their interactions as they traverse matter. They deposit their energy in a non-uniform way, in contrast to photons and the result is the high level of ionisation clustering due to the increased LET (Fig. 2). The heavy particles' energy to traversing distance curve forms a peak, known as Bragg Peak. Thus, when targeting a tumour they tend to spare more healthy tissue. Ion therapy efficacy varies with the accelerated ion type. A critical characteristic of ion radiations is their relatively higher LET with heavier particles to have greater LET values; LET increases when particles are decelerated by their interaction with matter; the distance before the Bragg Peak depends on

Table 4. Reported cell death responses after high-LET radiation

| Radiation	Dose	Biological system	Cell death response	Ref
Protons or ^{60}Co photons	4 Gy	Cancer stem cells (CSC)-enriched cells from paclitaxel-resistant human H460 and A549 cell lines	Increased apoptosis with protons vs photons	(Ref. 159)
26.7 MeV Protons or 5 MeV Linac photons	5–40 Gy	PC3 and MCF7, Ca301D cell lines	Increased apoptosis with protons vs photons	(Ref. 141)
62 MeV Protons or ^{60}Co photons	8–24 Gy	Human HTB140 melanoma cells	Increased apoptosis with protons vs photons	(Refs 166, 167)
Protons or ^{60}Co photons	1 Gy	Mice bone marrow and thymic cortex	Increased apoptosis with protons vs photons	(Ref. 168)
		Mice spleen (white pulp)	Increased cell death with photons vs protons	
60 MeV Protons vs 250 kVp X-rays	0.3–4.0 Gy	Human peripheral blood lymphocytes	Increased cell death through necrosis with protons vs photons	(Ref. 161)
200 MeV Protons or 6 MV X-rays	4 Gy	HNSCC cell lines: HPV-negative (SqCC/Y1 and HN5), HPV-positive (UPCI-SCC-154 and UMSCC-47)	Same levels of apoptosis and necrosis	(Ref. 162)
			Increased senescence and mitotic catastrophe with protons	
4.5 MeV FLASH protons (LET = 10 keV/μm)	20 Gy Dose rates: 0.05 Gy/s, 1000 Gy/s	Normal human lung fibroblasts (IMR90)	Reduced senescence with 1000 Gy/s dose rate compared to 0.05 Gy/s	(Ref. 163)
5-6 MeV FLASH protons	~10–40 Gy Dose rate: ~10^9 Gy/s	Normal mouse embryonic fibroblast cells (hypoxic and normoxic condition)	Increased apoptosis (early and late) and necrosis in both normoxic and hypoxic condition after FLASH IR vs conventional IR	(Ref. 164)
			Reduced apoptosis and necrosis in hypoxic compared to normoxic condition after FLASH IR	
18.3 MeV/u Carbon ions (LET = 108 KeV/μm)	6 Gy Dose rate: 1 Gy/s	Human glioma cells (NP-2)	Induced cell death mostly through apoptosis and autophagy	(Ref. 142)
			Further induction of cellular senescence	
160 or 290 MeV/u Carbon ions (LET = 75 KeV/μm) or 50 kVp X-rays (LET = 30 KeV/μm)	2 or 4 Gy	Human glioblastoma cells (SHG44) and HeLa cells	Increased autophagic effect with Carbon ions vs X-rays and in a LET-dependent manner	(Ref. 169)
			Inhibition of autophagy increases apoptosis	
9.8 MeV/u Carbon ions (LET = 184 keV/μm)	3–10 Gy	p53-mutated HNSCC cell line (laryngeal squamous cell carcinoma (SQ20B))	Induction of mitotic catastrophe and delayed apoptosis (resistance in apoptosis)	(Refs 170, 171)
			In a smaller extent, cell cycle re-entry and proliferation after IR	
9.8 MeV/u Carbon ions (LET = 184 keV/μm)	3–10 Gy	p53-mutated HNSCC cell line (tongue squamous cell carcinoma (SCC61))	Cell death mainly through apoptosis	(Refs 170, 171)
122.4–136.9 MeV/u (LET = 101 keV/ μm or 141.4–160.9 MeV/u (LET = 154 keV/ μm) or 320 kV X-rays	Carbon and oxygen ion: 1–3 Gy X-rays: 2 Gy with 1 Gy/min dose rate	Human oesophageal AC cell lines (OE19, OE33) and human oesophageal SCC lines (KYSE270, KYSE410)	Increased levels of apoptosis with ^{12}C and ^{16}O compared to photons	(Ref. 172)
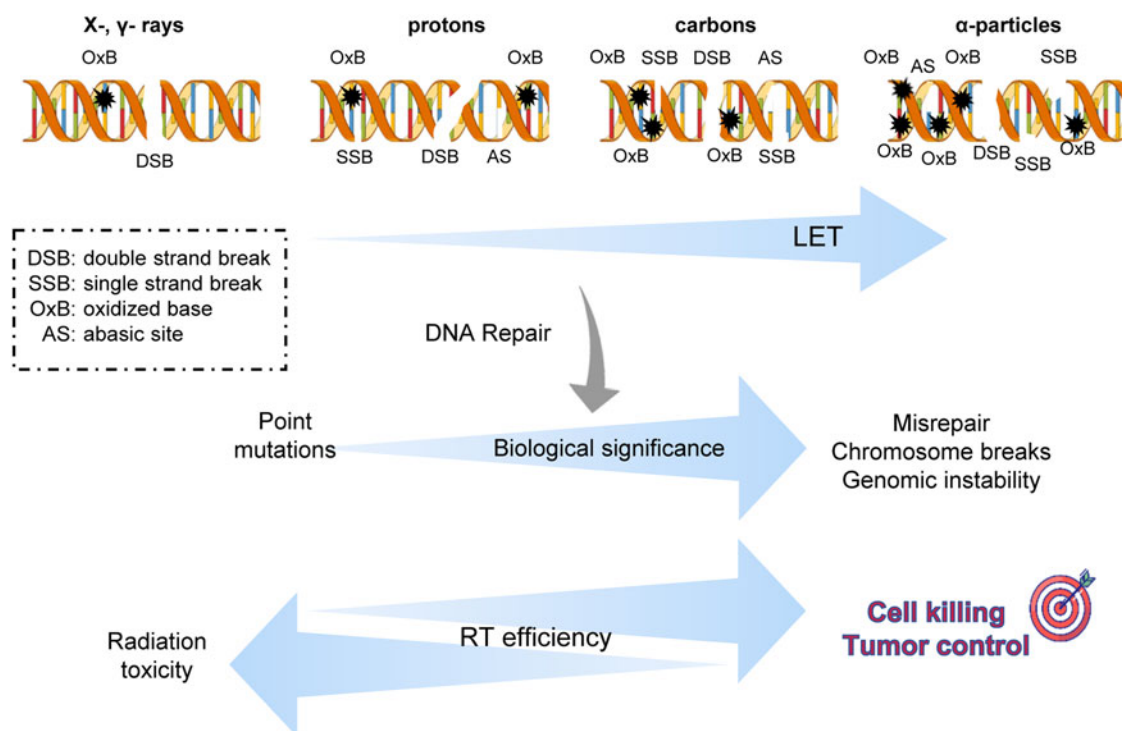
Fig. 2. Biological significance of complex DNA damage induced by high-LET radiation therapy. As the linear energy transfer increases the potency of particle radiation therapies against cancer cells increases due to a higher level of damage complexity that is DNA lesions in clustered form. But more research is needed towards the wide spectrum of biological response not only to tumour cells but normal cells usually receiving smaller doses.

their initial energy; a superposition of ions within a range of well-defined energy values forms the so-called SOBP that is used in the clinic.

Proton radiotherapy is the most widespread particle-RT in a clinic. Proton RT can be combined with chemotherapeutic agents, likely increasing efficacy and potentially reducing acute adverse events. Another emerging modality is FLASH RT where ultra-high dose rates appear to spare normal tissues to a higher extent than conventional radiation doses, though the precise mechanism it achieves this is currently unknown. Carbon ions allow better tolerance of radiosensitive organs, since they are characterised by a steeper dose distribution area with minimal penumbra compared to protons. α-particles emitted from radionuclides endoscopically placed near the tumour constituting brachytherapy. Another modality exploiting α-particles' high-LET is the one that we called herein as 'Nuclear radiotherapy', which is a type of combinatorial particle RT that involves molecule targets that have to be administrated in the tumour area. Nuclear reactions take place and their products, usually α-particles, have higher LET than the incident beam. The efficacy of nuclear RT is limited by a nuclear reaction cross section that is at least 10^4 times smaller than the corresponding one for the ionisation process.

In conclusion, there are several theoretical appealing features of medium-to-high LET particle radiation therapies as anti-tumour modalities. However, it is evident that, more thorough research is needed for a better understanding of the basic biological mechanisms underlying their effectiveness and for their safer application in the clinic so as to ensure maximum tumour control and minimisation of possible normal tissue toxicity in long term cancer survivors.

References

1. **Somosy Z** (2000) Radiation response of cell organelles. *Micron* **31**, 165–181.
2. **Tremi I et al.** (2021) A guide for using transmission electron microscopy for studying the radiosensitizing effects of gold nanoparticles *in vitro*. *Nanomaterials* **11**, 859.
3. **Nikjoo H et al.** (1998) Track structure in radiation biology: theory and applications. *International Journal of Radiation Biology* **73**, 355–364.
4. **Nikjoo H** (2003) Radiation track and DNA damage. *Iranian Journal of Radiation Research* **1**, 3–16.
5. **Schardt D, Elsaesser T and Schulz-Ertner D** (2010) Heavy-ion tumor therapy: physical and radiobiological benefits. *Reviews of Modern Physics* **82**, 383–425.
6. **Watanabe R, Rahmanian S and Nikjoo H** (2015) Spectrum of radiation-induced clustered non-DSB damage – A Monte Carlo track structure modeling and calculations. *Radiation Research* **183**, 525–540.
7. **Baiocco G et al.** (2016) The origin of neutron biological effectiveness as a function of energy. *Scientific Reports* **6**, 34033.

8. **Hada M and Georgakilas AG** (2008) Formation of clustered DNA damage after high-LET irradiation: a review. *Journal of Radiation Research* **49**, 203–210.

9. **Georgakilas AG, O'Neill P and Stewart RD** (2013) Induction and repair of clustered DNA lesions: what do we know so far? *Radiation Research* **180**, 100–109.

10. **Iliakis G, Mladenov E and Mladenova V** (2019) Necessities in the processing of DNA double-strand breaks and their effects on genomic instability and cancer. *Cancers* **11**, 1671.

11. **Murmann-Konda T** *et al.* (2021) Analysis of chromatid-break-repair detects a homologous recombination to non-homologous end-joining switch with increasing load of DNA double-strand breaks. *Mutation Research. Genetic Toxicology and Environmental Mutagenesis* **867**, 503372.

12. **Abbotts R and Wilson DM III** (2017) Coordination of DNA single-strand break repair. *Free Radical Biology & Medicine* **107**, 228–244.

13. **Yatagai F** (2004) Mutations induced by heavy charged particles. *Biological Sciences in Space* **18**, 224–234.

14. **Kawata T** *et al.* (2004) Chromosome aberrations induced by high-LET radiations. *Biological Sciences in Space* **18**, 216–223.

15. **Schipler A and Iliakis G** (2013) DNA double-strand–break complexity levels and their possible contributions to the probability for error-prone processing and repair pathway choice. *Nucleic Acids Research* **41**, 7589–7605.

16. **Averbeck NB** *et al.* (2014) DNA end resection is needed for the repair of complex lesions in G1-phase human cells. *Cell Cycle* **13**, 2509–2516.

17. **Grabarz A** *et al.* (2012) Initiation of DNA double-strand break repair: signaling and single-stranded resection dictate the choice between homologous recombination, non-homologous end-joining and alternative end-joining. *American Journal of Cancer Research* **2**, 249–268.

18. **Averbeck NB** *et al.* (2016) Efficient rejoining of DNA double-strand breaks despite increased cell-killing effectiveness following spread-out Bragg peak carbon-Ion irradiation. *Frontiers in Oncology* **6**, 28.

19. **Nickoloff JA** (2021) Toward greater precision in cancer radiotherapy. *Cancer Research* **81**, 3156–3157.

20. **Seidl C** (2014) Radioimmunotherapy with α-particle-emitting radionuclides. *Immunotherapy* **6**, 431–458.

21. **Vanderwaeren L** *et al.* (2021) Clinical progress in proton radiotherapy: biological unknowns. *Cancers* **13**, 604.

22. **Wilson RR** (1946) Radiological use of fast protons. *Radiology* **47**, 487–491.

23. **Lawrence JH** *et al.* (1958) Pituitary irradiation with high-energy proton beams: a preliminary report. *Cancer Research* **18**, 121–134.

24. **Yuan TZ, Zhan ZJ and Qian CN** (2019) New frontiers in proton therapy: applications in cancers. *Cancer Communications* **39**, 61.

25. **Baumann BC** *et al.* (2020) Comparative effectiveness of proton vs photon therapy as part of concurrent chemoradiotherapy for locally advanced cancer. *JAMA Oncology* **6**, 237–246.

26. **Hughes JR and Parsons JL** (2020) FLASH Radiotherapy: current knowledge and future insights using proton-beam therapy. *International Journal of Molecular Sciences* **21**, 6492.

27. **Favaudon V** *et al.* (2014) Ultrahigh dose-rate FLASH irradiation increases the differential response between normal and tumor tissue in mice. *Science Translational Medicine* **6**, 245ra93.

28. **Chabi S** *et al.* (2021) Ultra-high-dose-rate FLASH and conventional-dose-rate irradiation differentially affect human acute lymphoblastic leukemia and normal hematopoiesis. *International Journal of Radiation Oncology Biology Physics* **109**, 819–829.

29. **Montay-Gruel P** *et al.* (2021) Hypofractionated FLASH-RT as an effective treatment against glioblastoma that reduces neurocognitive side effects in mice. *Clinical Cancer Research* **27**, 775–784.

30. **Bourhis J** *et al.* (2019) Treatment of a first patient with FLASH-radiotherapy. *Radiotherapy & Oncology* **139**, 18–22.

31. **Vozenin MC** *et al.* (2019) The advantage of FLASH radiotherapy confirmed in mini-pig and cat-cancer patients. *Clinical Cancer Research* **25**, 35–42.

32. **Kim MM** *et al.* (2021) Comparison of FLASH proton entrance and the spread-out Bragg peak dose regions in the sparing of mouse intestinal crypts and in a pancreatic tumor model. *Cancers (Basel)* **13**, 4244.

33. **Velalopoulou A** *et al.* (2021) FLASH proton radiotherapy spares normal epithelial and mesenchymal tissues while preserving sarcoma response. *Cancer Research* **81**, 4808–4821.

34. **Diffenderfer ES** *et al.* (2020) Design, implementation, and *in vivo* validation of a novel proton FLASH radiation therapy system. *International Journal of Radiation Oncology Biology Physics* **106**, 440–448.

35. **Malouff TD** *et al.* (2020) Carbon ion therapy: a modern review of an emerging technology. *Frontiers in Oncology* **10**, 82.

36. **Brown A and Suit H** (2004) The centenary of the discovery of the Bragg peak. *Radiotherapy & Oncology* **73**, 265–268.

37. **Rackwitz T and Debus J** (2019) Clinical applications of proton and carbon ion therapy. *Seminars in Oncology* **46**, 226–232.

38. **Mohamad O** *et al.* (2017) Carbon ion radiotherapy: a review of clinical experiences and preclinical research, with an emphasis on DNA damage/repair. *Cancers* **9**, 66.

39. **Durante M and Loeffler JS** (2010) Charged particles in radiation oncology. *Nature Reviews, Clinical Oncology* **7**, 37–43.

40. **Kamada T** *et al.* (2015) Carbon ion radiotherapy in Japan: an assessment of 20 years of clinical experience. *The Lancet, Oncology* **16**, e93–e100.

41. **Tsujii H and Kamada T** (2012) A review of update clinical results of carbon ion radiotherapy. *Japanese Journal of Clinical Oncology* **42**, 670–685.

42. **Imada H** *et al.* (2010) Comparison of efficacy and toxicity of short-course carbon ion radiotherapy for hepatocellular carcinoma depending on their proximity to the porta hepatis. *Radiotherapy & Oncology* **96**, 231–235.

43. **Raju MR and Carpenter SG** (1978) A heavy particle comparative study. Part IV: acute and late reactions. *The British Journal of Radiology* **51**, 720–727.

44. **Ebner DK and Kamada T** (2016) The emerging role of carbon-ion radiotherapy. *Frontiers in Oncology* **6**, 140.

45. **Shinoto M** *et al.* (2016) Carbon ion radiation therapy with concurrent gemcitabine for patients with locally advanced pancreatic cancer. *International Journal of Radiation Oncology Biology Physics* **95**, 498–504.

46. **Kaganovich ID** *et al.* (2005) Ionization cross-sections for ion–atom collisions in high-energy ion beams. *Nuclear Instruments and Methods in Physics Research Section A: Accelerators, Spectrometers, Detectors and Associated Equipment* **544**, 91–97.

47. **Tawara H and Kato T** (1987) Total and partial ionization cross sections of atoms and ions by electron impact. *Atomic Data and Nuclear Data Tables* **36**, 167–353.

48. **Malouff TD** *et al.* (2021) Boron neutron capture therapy: a review of clinical applications. *Frontiers in Oncology* **11**, 601820.

49. **Bláha P** *et al.* (2021) The proton-boron reaction increases the radiobiological effectiveness of clinical low- and high-energy proton beams: novel experimental evidence and perspectives. *Frontiers in Oncology* **11**, 682647.

50. **Maliszewska-Olejniczak K** *et al.* (2021) Molecular mechanisms of specific cellular DNA damage response and repair induced by the mixed radiation field during boron neutron capture therapy. *Frontiers in Oncology* **11**, 676575.

51. **Ajzenberg-Selove F** (1975) Energy levels of light nuclei $A = 11$?12. Nuclear physics. *A, Nuclear and Hadronic Physics* **248**, 1–152.

52. **Stave S** *et al.* (2011) Understanding the B11(p,α)$\alpha\alpha$ reaction at the 0.675 MeV resonance. *Physics Letters B* **696**, 26–29.

53. **Barth RF, Mi P and Yang W** (2018) Boron delivery agents for neutron capture therapy of cancer. *Cancer Commun (Lond)* **38**, 35.

54. **Barth RF, Zhang Z and Liu T** (2018) A realistic appraisal of boron neutron capture therapy as a cancer treatment modality. *Cancer Commun (Lond)* **38**, 36.

55. **Barth RF** *et al.* (2005) Boron neutron capture therapy of cancer: current status and future prospects. *Clinical Cancer Research* **11**, 3987–4002.

56. **Miyatake S** *et al.* (2016) Boron neutron capture therapy for malignant brain tumors. *Neurol Med Chir (Tokyo)* **56**, 361–371.

57. **Wang L-W** *et al.* (2018) Clinical trials for treating recurrent head and neck cancer with boron neutron capture therapy using the Tsing-Hua open pool reactor. *Cancer Communications* **38**, 37.

58. **Hiratsuka J** *et al.* (2018) Boron neutron capture therapy for vulvar melanoma and genital extramammary Paget's disease with curative responses. *Cancer Communications* **38**, 38.

59. **De Stasio G** *et al.* (2001) Gadolinium in human glioblastoma cells for gadolinium neutron capture therapy. *Cancer Research* **61**, 4272–4277.

60. **Martin RF** *et al.* (1989) Induction of DNA double-strand breaks by 157Gd neutron capture. *Pigment Cell Research* **2**, 330–332.

61. **Shih JL and Brugger RM** (1992) Gadolinium as a neutron capture therapy agent. *Medical Physics* **19**, 733–744.

62. **Nomoto T** *et al.* (2020) Poly(vinyl alcohol) boosting therapeutic potential of p-boronophenylalanine in neutron capture therapy by modulating metabolism. *Science Advances* **6**, eaaz1722.

63. **Fukuda H** *et al.* (1999) Pharmacokinetics of 10B-p-boronophenylalanine in tumours, skin and blood of melanoma patients: a study of boron neutron capture therapy for malignant melanoma. *Melanoma Research* **9**, 75–83.

64. **Farr LE** *et al.* (1954) Neutron capture therapy with boron in the treatment of glioblastoma multiforme. *The American Journal of Roentgenology, Radium Therapy, and Nuclear Medicine* **71**, 279–293.

65. **Godwin JT** *et al.* (1955) Pathological study of eight patients with glioblastoma multiforme treated by neutron capture therapy using boron 10. *Cancer* **8**, 601–615.

66. **Goodman JH** *et al.* (2000) Boron neutron capture therapy of brain tumors: biodistribution, pharmacokinetics, and radiation dosimetry sodium borocaptate in patients with gliomas. *Neurosurgery* **47**, 608–621. discussion 21-2.

67. **Coderre JA** *et al.* (1998) Biodistribution of boronophenylalanine in patients with glioblastoma multiforme: boron concentration correlates with tumor cellularity. *Radiation Research* **149**, 163–170.

68. **Chanana AD** *et al.* (1999) Boron neutron capture therapy for glioblastoma multiforme: interim results from the phase I/II dose-escalation studies. *Neurosurgery* **44**, 1182–1192. discussion 92-3.

69. **Henriksson R** *et al.* (2008) Boron neutron capture therapy (BNCT) for glioblastoma multiforme: a phase II study evaluating a prolonged high-dose of boronophenylalanine (BPA). *Radiotherapy & Oncology* **88**, 183–191.

70. **Kawabata S** *et al.* (2009) Survival benefit from boron neutron capture therapy for the newly diagnosed glioblastoma patients. *Applied Radiation and Isotopes* **67**, S15–S18.

71. **Miyatake S** *et al.* (2007) Boron neutron capture therapy for malignant tumors related to meningiomas. *Neurosurgery* **61**, 82–90. discussion 90-1.

72. **Kankaanranta L** *et al.* (2012) Boron neutron capture therapy in the treatment of locally recurred head-and-neck cancer: final analysis of a phase I/II trial. *International Journal of Radiation Oncology Biology Physics* **82**, e67–e75.

73. **Suzuki M** *et al.* (2014) Boron neutron capture therapy outcomes for advanced or recurrent head and neck cancer. *Journal of Radiation Research* **55**, 146–153.

74. **Kato I** *et al.* (2009) Effectiveness of boron neutron capture therapy for recurrent head and neck malignancies. *Applied Radiation and Isotopes* **67**, S37–S42.

75. **Koivunoro H** *et al.* (2019) Boron neutron capture therapy for locally recurrent head and neck squamous cell carcinoma: an analysis of dose response and survival. *Radiotherapy & Oncology* **137**, 153–158.

76. **Wang LW** *et al.* (2014) Fractionated BNCT for locally recurrent head and neck cancer: experience from a phase I/II clinical trial at tsing Hua open-pool reactor. *Applied Radiation and Isotopes* **88**, 23–27.

77. **Suzuki M** *et al.* (2008) A novel concept of treatment of diffuse or multiple pleural tumors by boron neutron capture therapy (BNCT). *Radiotherapy & Oncology* **88**, 192–195.

78. **Futamura G** *et al.* (2014) A case of radiation-induced osteosarcoma treated effectively by boron neutron capture therapy. *Radiation Oncology* **9**, 237.

79. **Menéndez PR** *et al.* (2009) BNCT For skin melanoma in extremities: updated Argentine clinical results. *Applied Radiation and Isotopes* **67**, S50–S53.

80. **González SJ** *et al.* (2004) First BNCT treatment of a skin melanoma in Argentina: dosimetric analysis and clinical outcome. *Applied Radiation and Isotopes* **61**, 1101–1105.

81. **Yong Z** *et al.* (2016) Boron neutron capture therapy for malignant melanoma: first clinical case report in China. *Chinese Journal of Cancer Research = Chung-kuo Yen Cheng Yen Chiu* **28**, 634–640.

82. **Nakagawa Y** *et al.* (2009) Clinical results of BNCT for malignant brain tumors in children. *Applied Radiation and Isotopes* **67**, S27–S30.

83. **Zhang X** *et al.* (2019) Assessment of long-term risks of secondary cancer in paediatric patients with brain tumours after boron neutron capture therapy. *Journal of Radiological Protection* **39**, 838–853.

84. **Kageji T** *et al.* (2015) Radiation-induced meningiomas after BNCT in patients with malignant glioma. *Applied Radiation and Isotopes* **106**, 256–259.

85. **Wittig A** *et al.* (2008) Uptake of two 10B-compounds in liver metastases of colorectal adenocarcinoma for extracorporeal irradiation with boron neutron capture therapy (EORTC trial 11001). *International Journal of Cancer* **122**, 1164–1171.

86. **Zonta A** *et al.* (2009) Extra-corporeal liver BNCT for the treatment of diffuse metastases: what was learned and what is still to be learned. *Applied Radiation and Isotopes* **67**, S67–S75.

87. **Sgouros G** (2019) α-Particle–emitter radiopharmaceutical therapy: resistance is futile. *Cancer Research* **79**, 5479.

88. **Yard BD** *et al.* (2019) Cellular and genetic determinants of the sensitivity of cancer to α-particle irradiation. *Cancer Research* **79**, 5640.

89. **Stewart RD** *et al.* (2011) Effects of radiation quality and oxygen on clustered DNA lesions and cell death. *Radiation Research* **176**, 587–602.

90. **Anand A** *et al.* (2020) Assessing radiographic response to (223)Ra with an automated bone scan index in metastatic castration-resistant prostate cancer patients. *Journal of Nuclear Medicine* **61**, 671–675.

91. **Darafsheh A** *et al.* (2021) Spread-out Bragg peak proton FLASH irradiation using a clinical synchrocyclotron: proof of concept and ion chamber characterization. *Medical Physics* **48**, 4472–4484.

92. **Kourkafas G** *et al.* (2021) FLASH Proton irradiation setup with a modulator wheel for a single mouse eye. *Medical Physics* **48**, 1839–1845.

93. **Nikjoo H** *et al.* (2016) Radiation track, DNA damage and response-a review. *Reports on Progress in Physics* **79**, 116601.

94. **Chatzipapas KP** *et al.* (2020) Ionizing radiation and complex DNA damage: quantifying the radiobiological damage using Monte Carlo simulations. *Cancers* **12**, 799.

95. **Kalospyros SA** *et al.* (2021) A mathematical radiobiological model (MRM) to predict Complex DNA damage and cell survival for ionizing particle radiations of varying quality. *Molecules* **26**, 840.

96. **McMahon SJ and Prise KM** (2021) A mechanistic DNA repair and survival model (Medras): applications to intrinsic radiosensitivity, relative biological effectiveness and dose-rate. *Frontiers in Oncology* **11**, 2319.

97. **Papakonstantinou D** *et al.* (2021) Using machine learning techniques for asserting cellular damage induced by high-LET particle radiation. *Radiation* **1**, 45–64.

98. **Zhao X** *et al.* (2020) Modeling double-strand breaks from direct and indirect action in a complete human genome single cell Geant4 model. *Biomedical Physics and Engineering Express* **6**, 065010.

99. **Mokari M** *et al.* (2018) A simulation approach for determining the spectrum of DNA damage induced by protons. *Physics in Medicine and Biology* **63**, 175003.

100. **Chan CC, Chen FH and Hsiao YY** (2021) Impact of hypoxia on relative biological effectiveness and oxygen enhancement ratio for a 62-MeV therapeutic proton beam. *Cancers (Basel)* **13**, 2997.

101. **Pater P** *et al.* (2016) Proton and light ion RBE for the induction of direct DNA double-strand breaks. *Medical Physics* **43**, 2131.

102. **Keta O** *et al.* (2021) DNA double-strand breaks in cancer cells as a function of proton linear energy transfer and its variation in time. *International Journal of Radiation Biology* **97**, 1229–1240.

103. **Luo WR** *et al.* (2020) Effects of indirect actions and oxygen on relative biological effectiveness: estimate of DSB inductions and conversions induced by therapeutic proton beams. *International Journal of Radiation Biology* **96**, 187–196.

104. **Ohsawa D** *et al.* (2021) DNA Strand break induction of aqueous plasmid DNA exposed to 30 MeV protons at ultra-high dose rate. *Journal of Radiation Research*, rrab114.

105. **Yokota Y** *et al.* (2007) Initial yields of DNA double-strand breaks and DNA fragmentation patterns depend on linear energy transfer in tobacco BY-2 protoplasts irradiated with helium, carbon and neon ions. *Radiation Research* **167**, 94–101.

106. **Heilmann J, Taucher-Scholz G and Kraft G** (1995) Induction of DNA double-strand breaks in CHO-K1 cells by carbon ions. *International Journal of Radiation Biology* **68**, 153–162.

107. **Shiina T** *et al.* (2013) Induction of DNA damage, including abasic sites, in plasmid DNA by carbon ion and X-ray irradiation. *Radiation and Environmental Biophysics* **52**, 99–112.

108. **Watanabe R** *et al.* (2011) Monte Carlo simulation of radial distribution of DNA strand breaks along the C and Ne ion paths. *Radiation Protection Dosimetry* **143**, 186–190.

109. **Macaeva E** *et al.* (2021) High-LET carbon and iron ions elicit a prolonged and amplified p53 signaling and inflammatory response compared to low-LET X-rays in human peripheral blood mononuclear cells. *Frontiers in Oncology* **11**, 768493.

110. **Urushibara A** *et al.* (2006) DNA Damage induced by the direct effect of He ion particles. *Radiation Protection Dosimetry* **122**, 163–165.

111. **Prise KM, Pullar CH and Michael BD** (1999) A study of endonuclease III-sensitive sites in irradiated DNA: detection of alpha-particle-induced oxidative damage. *Carcinogenesis* **20**, 905–909.

112. **Claesson K** *et al.* (2011) RBE Of α-particles from (211) At for complex DNA damage and cell survival in relation to cell cycle position. *International Journal of Radiation Biology* **87**, 372–384.

113. **Roots R** *et al.* (1990) The formation of strand breaks in DNA after high-LET irradiation: a comparison of data from in vitro and cellular systems. *International Journal of Radiation Biology* **58**, 55–69.

114. **Fulford J** *et al.* (2001) Yields of SSB and DSB induced in DNA by Al(K) ultrasoft X-rays and alpha-particles: comparison of experimental and simulated yields. *International Journal of Radiation Biology* **77**, 1053–1066.

115. **Gorgoulis VG** *et al.* (2018) Integrating the DNA damage and protein stress responses during cancer development and treatment. *The Journal of Pathology* **246**, 12–40.

116. **Chatgilialoglu C** *et al.* (2014) Lipid geometrical isomerism: from chemistry to biology and diagnostics. *Chemical Reviews* **114**, 255–284.

117. **Sridharan DM** *et al.* (2015) Understanding cancer development processes after HZE-particle exposure: roles of ROS, DNA damage repair and inflammation. *Radiation Research* **183**, 1–26. 26.

118. **Zhao L** *et al.* (2020) The determinant of DNA repair pathway choices in ionising radiation-induced DNA double-strand breaks. *BioMed Research International* **2020**, 4834965.

119. **Shrivastav M, De Haro LP and Nickoloff JA** (2008) Regulation of DNA double-strand break repair pathway choice. *Cell Research* **18**, 134–147.

120. **Takahashi A** *et al.* (2014) Nonhomologous end-joining repair plays a more important role than homologous recombination repair in defining radiosensitivity after exposure to high-LET radiation. *Radiation Research* **182**, 338–344.

121. **Okayasu R** *et al.* (2006) Repair of DNA damage induced by accelerated heavy ions in mammalian cells proficient and deficient in the non-homologous End-joining pathway. *Radiation Research* **165**, 59–67. 9.

122. **Sridharan DM** *et al.* (2012) Increased Artemis levels confer radioresistance to both high and low LET radiation exposures. *Radiation Oncology* **7**, 96.

123. **Singh SK** *et al.* (2013) Reduced contribution of thermally labile sugar lesions to DNA double-strand break formation after exposure to heavy ions. *Radiation Oncology* **8**, 77.

124. **Faria Z** *et al.* (2010) Homologous recombination contributes to the repair of DNA double-strand breaks induced by high-energy iron ions. *Radiation Research* **173**, 27–39.

125. **Grosse N** *et al.* (2014) Deficiency in homologous recombination renders mammalian cells more sensitive to proton versus photon irradiation. *International Journal of Radiation Oncology Biology Physics* **88**, 175–181.

126. **Rostek C** *et al.* (2008) Involvement of homologous recombination repair after proton-induced DNA damage. *Mutagenesis* **23**, 119–129.

127. **Zhou X** *et al.* (2013) DNA-PKcs Inhibition sensitizes cancer cells to carbon-Ion irradiation via telomere capping disruption. *PLoS One* **8**, e72641.

128. **Ariungerel G** *et al.* (2015) The major DNA repair pathway after both proton and carbon-Ion radiation is NHEJ, but the HR pathway is more relevant in carbon ions. *Radiation Research* **183**, 345–356.

129. **Kondo N** *et al.* (2016) DNA Damage induced by boron neutron capture therapy is partially repaired by DNA ligase IV. *Radiation and Environmental Biophysics* **55**, 89–94.

130. **Rodriguez C** *et al.* (2018) In vitro studies of DNA damage and repair mechanisms induced by BNCT in a poorly differentiated thyroid carcinoma cell line. *Radiation and Environmental Biophysics* **57**, 143–152.

131. **Ghosh S** *et al.* (2011) DNA Damage response signaling in lung adenocarcinoma A549 cells following gamma and carbon beam irradiation. *Mutation Research/Fundamental and Molecular Mechanisms of Mutagenesis* **716**, 10–19.

132. **Rydberg B** *et al.* (2005) Dose-dependent Misrejoining of radiation-induced DNA double-strand breaks in human fibroblasts: experimental and theoretical study for high- and low-LET radiation. *Radiation Research* **163**, 526–534. 9.

133. **Autsavapromporn N** *et al.* (2013) Participation of gap junction communication in potentially lethal damage repair and DNA damage in human fibroblasts exposed to low- or high-LET radiation. *Mutation Research/Genetic Toxicology and Environmental Mutagenesis* **756**, 78–85.

134. **Saha J** *et al.* (2014) Biological characterization of low-energy ions with high-energy deposition on human cells. *Radiation Research* **182**, 282–291.

135. **Facoetti A** (2020) [The risk of second radiation-induced cancer from hadrontherapy compared to traditional radiotherapy]. *Giornale Italiano di Medicina del Lavoro ed Ergonomia* **42**, 252–256.

136. **Okumura K** *et al.* (2012) Relative biological effects of neutron mixed-beam irradiation for boron neutron capture therapy on cell survival and DNA double-strand breaks in cultured mammalian cells. *Journal of Radiation Research* **54**, 70–75.

137. **Cheng L** *et al.* (2018) Simultaneous induction of dispersed and clustered DNA lesions compromises DNA damage response in human peripheral blood lymphocytes. *PLoS ONE* **13**, e0204068.

138. **Golden E** *et al.* (2012) The convergence of radiation and immunogenic cell death signaling pathways. *Frontiers in Oncology* **2**, 88.

139. **Eriksson D and Stigbrand T** (2010) Radiation-induced cell death mechanisms. *Tumor Biology* **31**, 363–372.

140. **Radford IR** *et al.* (1994) Radiation response of mouse lymphoid and myeloid cell lines. Part II. Apoptotic death is shown by all lines examined. *International Journal of Radiation Biology* **65**, 217–227.

141. **Di Pietro C** *et al.* (2006) Cellular and molecular effects of protons: apoptosis induction and potential implications for cancer therapy. *Apoptosis* **11**, 57–66.

142. **Jinno-Oue A** *et al.* (2010) Irradiation with carbon Ion beams induces apoptosis, autophagy, and cellular senescence in a human glioma-derived cell line. *International Journal of Radiation Oncology Biology Physics* **76**, 229–241.

143. **Rahmanian N, Hosseinimehr SJ and Khalaj A** (2016) The paradox role of caspase cascade in ionizing radiation therapy. *Journal of Biomedical Science* **23**, 88.

144. **Fabbrizi MR and Parsons JL** (2022) Cell death mechanisms in head and neck cancer cells in response to low and high-LET radiation. *Expert Reviews in Molecular Medicine* **24**, e2.

145. **Campisi J and d'Adda di Fagagna F** (2007) Cellular senescence: when bad things happen to good cells. *Nature Reviews Molecular Cell Biology* **8**, 729–740.

146. **Alvarado-Ortiz E** *et al.* (2021) Mutant p53 gain-of-function: role in cancer development, progression, and therapeutic approaches. *Frontiers in Cell and Developmental Biology* **8**, 607670.

147. **Kastenhuber ER and Lowe SW** (2017) Putting p53 in context. *Cell* **170**, 1062–178.

148. **Rödel F** *et al.* (2005) Survivin as a radioresistance factor, and prognostic and therapeutic target for radiotherapy in rectal cancer. *Cancer Research* **65**, 4881–4887.

149. **Cuddihy AR and Bristow RG** (2004) The p53 protein family and radiation sensitivity: yes or no? *Cancer and Metastasis Reviews* **23**, 237–257.

150. **MacDonald SM** (2016) Chapter 67 – central nervous system tumors in children. In Gunderson LL and Tepper JE (eds), *Clinical Radiation Oncology*, 4th Edn. Philadelphia: Elsevier, pp. 1389–1402.e3.

151. **Brown JM and Wouters BG** (1999) Apoptosis, p53, and tumor cell sensitivity to anticancer agents. *Cancer Research* **59**, 1391–1399.

152. **Eliopoulos AG, Havaki S and Gorgoulis VG** (2016) DNA Damage response and autophagy: a meaningful partnership. *Frontiers in Genetics* **7**, 204.

153. **Wu WKK** *et al.* (2012) The autophagic paradox in cancer therapy. *Oncogene* **31**, 939–953.

154. **Paglin S** *et al.* (2001) A novel response of cancer cells to radiation involves autophagy and formation of acidic vesicles. *Cancer Research* **61**, 439–444.

155. **Palumbo S and Comincini S** (2013) Autophagy and ionizing radiation in tumors: the "survive or not survive" dilemma. *Journal of Cellular Physiology* **228**, 1–8.

156. **Gorgoulis V** *et al.* (2019) Cellular senescence: defining a path forward. *Cell* **179**, 813–827.

157. **Spratt DE** *et al.* (2016) Recurrence patterns and second primary lung cancers after stereotactic body radiation therapy for early-stage non–small-cell lung cancer: implications for surveillance. *Clinical Lung Cancer* **17**, 177–183. e2.

158. **Liao EC** *et al.* (2014) Radiation induces senescence and a bystander effect through metabolic alterations. *Cell Death & Disease* **5**, e1255–e1e55.

159. **Zhang X** *et al.* (2013) Therapy-resistant cancer stem cells have differing sensitivity to photon versus proton beam radiation. *Journal of Thoracic Oncology* **8**, 1484–1491.

160. **Ristic-Fira AM** *et al.* (2007) Response of a human melanoma cell line to low and high ionizing radiation. *Annals of the New York Academy of Sciences* **1095**, 165–174.

161. **Miszczyk J** *et al.* (2018) Do protons and X-rays induce cell-killing in human peripheral blood lymphocytes by different mechanisms? *Clinical and Translational Radiation Oncology* **9**, 23–29.

162. **Wang L et al.** (2019) Proton versus photon radiation–induced cell death in head and neck cancer cells. *Head & Neck* **41**, 46–55.

163. **Buonanno M, Grilj V and Brenner DJ** (2019) Biological effects in normal cells exposed to FLASH dose rate protons. *Radiotherapy and Oncology* **139**, 51–55.

164. **Han J et al.** (2021) Ultra-high dose rate FLASH irradiation-induced radio-resistance of normal fibroblast cells can be enhanced by hypoxia and mitochondrial dysfunction resulting from loss of cytochrome C. *Frontiers in Cell and Developmental Biology* **9**, 672929.

165. **Rock KL and Kono H** (2008) The inflammatory response to cell death. *Annual Review of Pathology* **3**, 99–126.

166. **Ristic-Fira AM et al.** (2007) Response of a human melanoma cell line to low and high ionizing radiation. *Annals of the New York Academy of Sciences* **1095**, 165–174.

167. **Petrović I et al.** (2006) Radiobiological analysis of human melanoma cells on the 62 MeV CATANA proton beam. *International Journal of Radiation Biology* **82**, 251–265.

168. **Finnberg N et al.** (2008) Gamma-radiation (GR) triggers a unique gene expression profile associated with cell death compared to proton radiation (PR) in mice in vivo. *Cancer Biology & Therapy* **7**, 2023–2033.

169. **Jin X et al.** (2015) Carbon ions induce autophagy effectively through stimulating the unfolded protein response and subsequent inhibiting Akt phosphorylation in tumor cells. *Scientific Reports* **5**, 1–10.

170. **Bertrand G et al.** (2014) Targeting head and neck cancer stem cells to overcome resistance to photon and carbon ion radiation. *Stem Cell Reviews* **10**, 114–126.

171. **Maalouf M et al.** (2009) Different mechanisms of cell death in radiosensitive and radioresistant p53 mutated head and neck squamous cell carcinoma cell lines exposed to carbon ions and x-rays. *International Journal of Radiation Oncology Biology Physics* **74**, 200–209.

172. **Hartfiel S et al.** (2019) Differential response of esophageal cancer cells to particle irradiation. *Radiation Oncology (London, England)* **14**, 119–119.

173. **Jin X et al.** (2014) Role of autophagy in high linear energy transfer radiation-induced cytotoxicity to tumor cells. *Cancer Science* **105**, 770–778.

174. **Gill MR et al.** (2017) Targeted radionuclide therapy in combined-modality regimens. *The Lancet. Oncology* **18**, e414–e423.

175. **Aghevlian S, Boyle AJ and Reilly RM** (2017) Radioimmunotherapy of cancer with high linear energy transfer (LET) radiation delivered by radionuclides emitting α-particles or auger electrons. *Advanced Drug Delivery Reviews* **109**, 102–118.

176. **Larson SM et al.** (2015) Radioimmunotherapy of human tumours. *Nature Reviews Cancer* **15**, 347–360.

177. **Witzig TE et al.** (2002) Randomized controlled trial of yttrium-90-labeled ibritumomab tiuxetan radioimmunotherapy versus rituximab immunotherapy for patients with relapsed or refractory low-grade, follicular, or transformed B-cell non-Hodgkin's lymphoma. *Journal of Clinical Oncology: Official Journal of the American Society of Clinical Oncology* **20**, 2453–2463.

178. **Kaminski MS et al.** (2001) Pivotal study of iodine I 131 tositumomab for chemotherapy-refractory low-grade or transformed low-grade B-cell non-Hodgkin's lymphomas. *Journal of Clinical Oncology* **19**, 3918–3928.

179. **Kręcisz P et al.** (2021) Radiolabeled peptides and antibodies in medicine. *Bioconjugate Chemistry* **32**, 25–42.

180. **Tan Z et al.** (2012) Significant systemic therapeutic effects of high-LET immunoradiation by 212Pb-trastuzumab against prostatic tumors of androgen-independent human prostate cancer in mice. *International Journal of Oncology* **40**, 1881–1888.

181. **Miederer M et al.** (2004) Treatment of neuroblastoma meningeal carcinomatosis with intrathecal application of α-emitting atomic nanogenerators targeting disialo-ganglioside GD2. *Clinical Cancer Research* **10**, 6985–6992.

182. **McDevitt MR et al.** (2001) Tumor therapy with targeted atomic nanogenerators. *Science* **294**, 1537–1540.

183. **Borchardt PE et al.** (2003) Targeted actinium-225 in vivo generators for therapy of ovarian cancer. *Cancer Research* **63**, 5084–5090.

184. **Zalutsky MR et al.** (1997) Tissue distribution and radiation dosimetry of astatine-211-labeled chimeric 81C6, an α-particle-emitting immunoconjugate. *Nuclear Medicine and Biology* **24**, 255–261.

185. **Song H et al.** (2009) Radioimmunotherapy of breast cancer metastases with α-particle emitter 225Ac: comparing efficacy with 213Bi and 90Y. *Cancer Research* **69**, 8941–8948.

186. **Eriksson SE et al.** (2013) Successful radioimmunotherapy of established syngeneic rat colon carcinoma with 211At-mAb. *EJNMMI Research* **3**, 23.

187. **Milenic DE et al.** (2005) α-particle radioimmunotherapy of disseminated peritoneal disease using a 212Pb-labeled radioimmunoconjugate targeting HER2. *Cancer Biotherapy and Radiopharmaceuticals* **20**, 557–568.

188. **Milenic DE et al.** (2007) Potentiation of high-LET radiation by gemcitabine: targeting HER2 with trastuzumab to treat disseminated peritoneal disease. *Clinical Cancer Research* **13**, 1926–1935.

189. **Milenic DE et al.** (2015) Evaluation of cetuximab as a candidate for targeted α-particle radiation therapy of HER1-positive disseminated intra-peritoneal disease. *mAbs* **7**, 255–264.

190. **Orozco JJ et al.** (2013) Anti-CD45 radioimmunotherapy using 211at with bone marrow transplantation prolongs survival in a disseminated murine leukemia model. *Blood* **121**, 3759–3767.

191. **Huneke RB et al.** (1992) Effective α-particle-mediated radioimmunotherapy of Murine Leukemia. *Cancer Research* **52**, 5818–5820.

192. **Costantini DL et al.** (2010) Antitumor effects and normal-tissue toxicity of111In-nuclear localization sequence-trastuzumab in Athymic mice bearing HER-positive human breast cancer xenografts. *Journal of Nuclear Medicine* **51**, 1084–1091.

193. **Zalutsky MR et al.** (2008) Clinical experience with α-particle-emitting 211 At: treatment of recurrent brain tumor patients with 211 At-labeled chimeric antitenascin monoclonal antibody 81C6. *Journal of Nuclear Medicine* **49**, 30–38.

194. **Andersson H et al.** (2009) Intraperitoneal α-particle radioimmunotherapy of ovarian cancer patients: pharmacokinetics and dosimetry of 211At-MX35 F(ab′)2 - A phase I study. *Journal of Nuclear Medicine* **50**, 1153–1160.

195. **Meredith R et al.** (2014) Dose escalation and dosimetry of first-in-human α radioimmunotherapy with 212Pb-TCMC-trastuzumab. *Journal of Nuclear Medicine* **55**, 1636–1642.

196. **Meredith RF et al.** (2014) Pharmacokinetics and imaging of 212Pb-TCMC-trastuzumab after intraperitoneal administration in ovarian cancer patients. *Cancer Biotherapy and Radiopharmaceuticals* **29**, 12–17.